

Nitrogen Fixation with Water Vapor by Nonequilibrium Plasma:
toward Sustainable Ammonia Production

Yury Gorbanev,* Elise Vervloessem, Anton Nikiforov, and Annemie Bogaerts

Cite This: *ACS Sustainable Chem. Eng.* 2020, 8, 2996–3004

Read Online

ACCESS |



Metrics & More



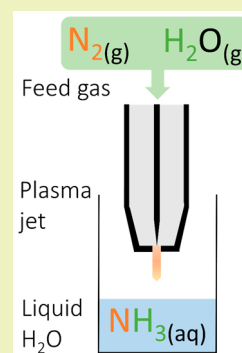
Article Recommendations



Supporting Information

ABSTRACT: Ammonia is a crucial nutrient used for plant growth and as a building block in the pharmaceutical and chemical industry, produced via nitrogen fixation of the ubiquitous atmospheric N_2 . Current industrial ammonia production relies heavily on fossil resources, but a lot of work is put into developing nonfossil-based pathways. Among these is the use of nonequilibrium plasma. In this work, we investigated water vapor as a H source for nitrogen fixation into NH_3 by nonequilibrium plasma. The highest selectivity toward NH_3 was observed with low amounts of added H_2O vapor, but the highest production rate was reached at high H_2O vapor contents. We also studied the role of H_2O vapor and of the plasma-exposed liquid H_2O in nitrogen fixation by using isotopically labeled water to distinguish between these two sources of H_2O . We show that added H_2O vapor, and not liquid H_2O , is the main source of H for NH_3 generation. The studied catalyst- and H_2 -free method offers excellent selectivity toward NH_3 (up to 96%), with energy consumption (ca. 95–118 MJ/mol) in the range of many plasma-catalytic H_2 -utilizing processes.

KEYWORDS: Nitrogen fixation, Ammonia, Nonequilibrium plasma, Plasma jet, Water vapor, Isotopically labeled water



INTRODUCTION

Nitrogen fixation is one of the utmost important tasks of sustainable chemistry. Both reduced and oxidized N_2 (NH_3 and NO_3^-/NO_2^-) are used as fertilizers in agriculture.¹ Approximately 80% of the globally produced NH_3 is used for plant growth.² Moreover, NH_3 is a commodity chemical used as an important building block for the production of pharmaceutical compounds, and it is also used in cleaning solutions, in the textile industry, as a greener fuel, as a deNOx agent in automotive industry, etc.^{3,4} Nitrogen fixation in part occurs naturally (e.g., by microorganisms^{1,5}), but this is by far not sufficient to meet the global demand.

The industrial production of NH_3 worldwide in 2018 reached 140 million tonnes.⁶ Most NH_3 production is realized via the Haber-Bosch process (HB), in which NH_3 is produced catalytically under high temperatures and extreme pressures from N_2 and H_2 . The nearly exclusive H source for HB is natural gas (fossil CH_4).^{6,7} Other, fossil-free routes for NH_3 production are very sought-after.² For example, electrochemical and photocatalytic reductions of N_2 are under investigation.^{8,9}

An attractive alternative is nonequilibrium plasma,¹⁰ i.e., ionized gas with the temperature of electrons dramatically exceeding the temperature of the gas molecules.^{11,12} Plasmas find their use in green and sustainable chemical processes, agriculture, and biomedical applications.^{13–17} They are also valuable in catalytic NH_3 production. A synergistic combination of cold plasma and catalysis affords higher reaction productivity in a way which is not achievable with conventional thermal catalysis,^{18,19} at least partly due to the excitation of the

strong bonds in N_2 by plasma,^{20,21} or the facile generation of H atoms.^{22,23} Plasma-catalytic nitrogen fixation typically proceeds in N_2/H_2 plasmas operating in a range from low (5–700 Pa) to atmospheric pressure.^{4,24,25}

A more direct alternative is H_2 -free, noncatalytic NH_3 synthesis by atmospheric pressure plasma in N_2/H_2O systems. A combined plasma-electrolytic system enables formation of NH_3 from H, which is generated from H_2O or H^+ .^{26,27} Another approach is the NH_3 formation via the direct interaction of air or N_2 plasma with H_2O .^{28–31} The latter enables simpler synthesis (and simpler reactors without the need for counter electrodes in liquids and additional electrolysis), including the immediate accumulation and potential storage of products in H_2O , the most benign solvent.³² Most of these works propose direct interaction of plasma with liquid water, despite recent insights suggesting that most of the reactive chemistry in plasma-liquid systems occurs in the gas (vapor) phase.^{33,34}

Here, we used for the first time a nonequilibrium atmospheric pressure plasma operated with N_2 containing H_2O vapor, in contact with liquid H_2O . We studied the induction of chemical products in the liquid phase as a function of H_2O vapor saturation of the feed gas, with special focus on NH_3 selectivity and production rate. In addition, to understand the underlying mechanisms, we evaluated the role

Received: December 31, 2019

Revised: January 30, 2020

Published: February 3, 2020

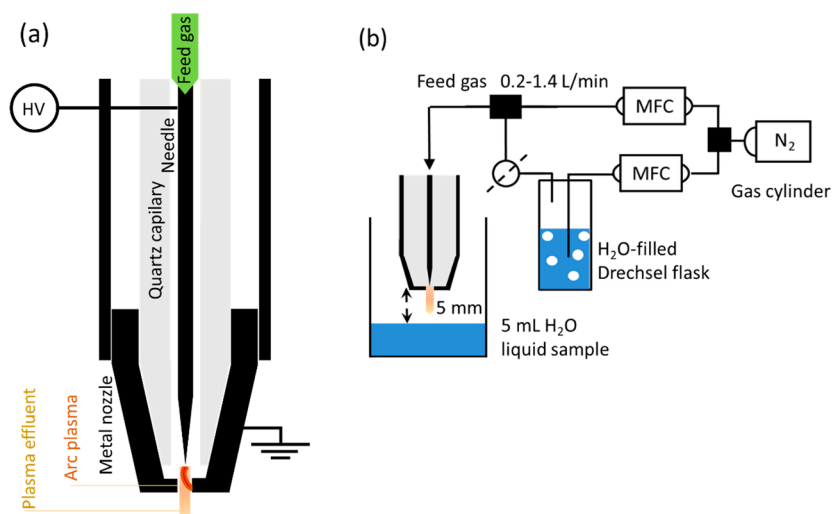


Figure 1. Experimental setup used in this work. (a) Schematic of the plasma jet; (b) plasma jet in direct contact with liquid contained in a glass reaction vessel.

of H₂O vapor in the feed gas and liquid H₂O by excluding the direct plasma-liquid interaction, and by discriminating between H₂O introduced with the feed gas and from the liquid sample, using isotopically labeled (D₂O) molecules.

EXPERIMENTAL SECTION

Plasma Setup Design and Characterization. We applied a plasma jet, typically used in biomedical applications, such as anticancer therapy³⁵ and synthesis of antibacterial nanomaterials.³⁶ The jet comprises a powered needle electrode inserted in a quartz capillary (OD 5 mm, ID 2 mm), contained in a metal tube. The feed gas flow was supplied into the capillary. The plasma was ignited inside a small cavity between the needle and the nozzle (ID 0.7 mm, volume ca. 0.5 mm³), with the nozzle serving as a ground electrode (Figure 1a) and the quartz tube as a dielectric spacer.

In our experiments, the plasma jet was connected to an N₂ gas cylinder. Partial saturation (i.e., % saturation) of the feed gas with H₂O vapor was achieved via splitting the N₂ flow. The H₂O content in N₂ was thus controlled by the flow rate of N₂ passing through the Drechsel flask filled with H₂O (Figure 1b). We have previously shown that a gas flow rate up to 2 L/min allows full saturation of the gas with H₂O vapor.³⁴ The gas flow was regulated using two mass flow controllers (MFCs) equipped with a microcomputer controller (Brooks Instruments 0254). The total N₂ flow rate was varied from 0.2 to 1.4 L/min. The concentration of H₂O vapor is quoted in percentage of the relative saturation at 19–21 °C (ambient temperature during the experiments), and in molar percentage as calculated from the relative saturation.^{34,37}

Plasma was ignited at a peak-to-peak voltage of ca. 1 kV, and a current of ca. 170 mA (Figure S1 in SI). The discharge was generated by connecting the secondary windings of a high frequency transformer to the system of electrodes separated by a small dielectric spacer. The waveforms of both voltage and current were close to sinusoidal and were governed by the primary winding and transformer characteristics and the high capacitance of the source, respectively. In contrast to a classical DBD plasma, the geometry used here allows the generation of a low current spark when the voltage reaches a value of ca. 0.5 kV. Taking into account the shape of the discharge (Figure S2), we consider the discharge mechanism to be similar to the phenomena occurring at a low current spark formation.³⁸ Thus, the jet operates in a pulsed spark mode. The calculated power deposited into the plasma was 0.1 W (Figure S1) regardless of the gas flow rate or vapor saturation.

Analysis of the optical emission spectra (as described in SI, T1) allowed to estimate the temperature of the plasma arc (Figure 1a) which was virtually the same for all N₂ gas flow rates and H₂O vapor

saturation (ca. 1350 ± 150 °C). However, the temperature of the plasma jet effluent was 2 orders of magnitude lower and dependent on the gas flow rate. Already at 3.4 mm away from the plasma jet, it was around 70 °C for 0.2 L/min and 35 °C for 1.4 L/min (±10 °C, see Table S1), as measured by Rayleigh scattering spectroscopy (Figure S3), and likely lower yet at a 5 mm distance, i.e., the position of the liquid H₂O surface in our N₂ fixation experiments. We also observed a mild increase of the plasma jet temperature as a function of time, which saturated within 10 min, likely due to reaching a thermal equilibrium with the surrounding atmosphere and the passing feed gas (Figure S4). These values indicate that our plasma setup is a nonequilibrium, nonthermal plasma.^{13,23} The temperature of both the plasma arc and the plasma effluent was higher than the ambient temperature, thus clearly indicating that the H₂O introduced into the plasma feed gas as vapor remained in the gas phase throughout the whole plasma reactive system.

Nitrogen Fixation Experiments. In a typical experiment, 5 mL of deionized H₂O was put in a glass reaction vessel and exposed to plasma for 10 min. The distance between the liquid surface and the plasma jet was 5 mm (Figure 1b). We also performed air-free experiments, for which the glass reaction vessel and the jet were positioned inside a gastight reactor^{33,39} to exclude the possible interference of ambient air. The reactor was flushed for 3 min with the feed gas, and then the plasma was ignited for 10 min (Figure S5). When performing experiments without a direct plasma-liquid contact, a glass tube (length ca. 330 mm, ID 5 mm, OD 7 mm) was pushed toward the plasma jet to cover the jet nozzle. The opposite end of the glass tube (ID 1 mm, OD 2 mm) was positioned 2 mm above the H₂O surface (5 mL) contained in a reaction vessel (Figure S6). Immediately after plasma exposure, the samples were collected and frozen until further analysis.

Liquid Analysis. We measured the concentrations of all chemical compounds by colorimetry. NH₃ concentrations were measured using the indophenol blue reaction.^{28,40} NH₂OH was assessed by colorimetry via reduction of Fe(III) to Fe(II) and subsequent complexation with 1,10-phenanthroline,⁴¹ and NH₂NH₂ via formation of an azo-dye in a reaction with 4-dimethylaminobenzaldehyde.⁴² The calibration curves and analysis details are found in the SI, Figure S7.

The concentrations of NO₃⁻ and NO₂⁻ were measured using the nitrate/nitrite kit based on the Griess method with nitrate reductase enzyme, and H₂O₂ was measured using titanium(IV) sulfate with the addition of NaN₃, as described previously.^{17,33,43}

Ambient and liquid temperature and pH values were measured using an Extech Instruments TM100 thermometer and a Mettler Toledo MP255 pH meter, respectively.

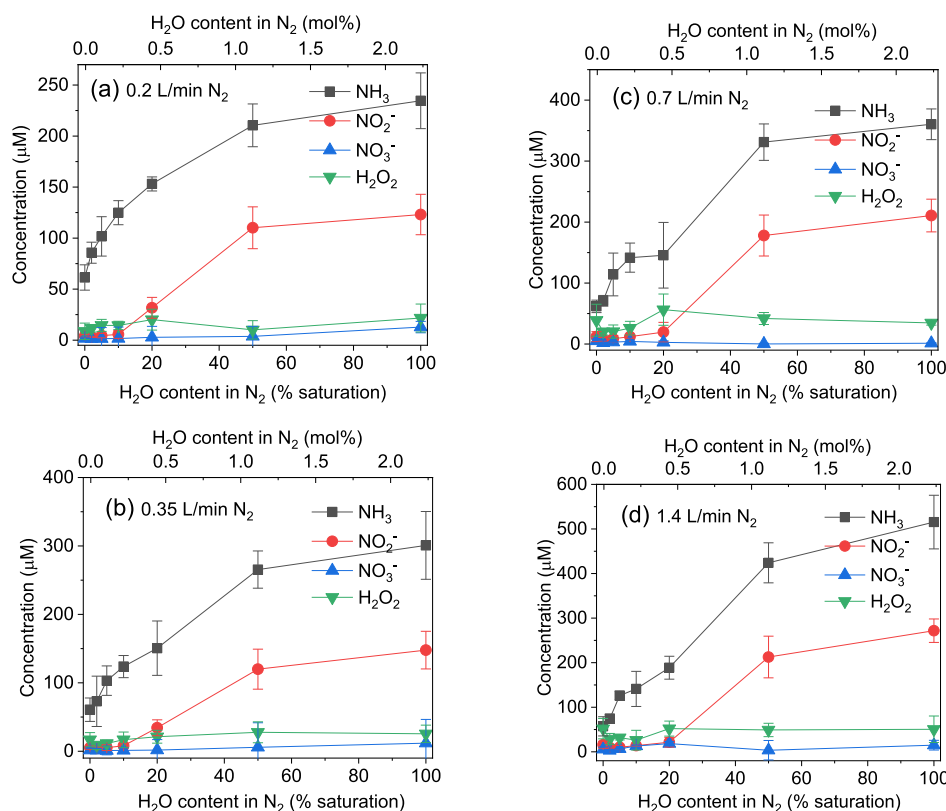


Figure 2. Concentration of produced NH_3 , NO_2^- , NO_3^- , and H_2O_2 in liquid H_2O as a function of H_2O vapor saturation for different N_2 flow rates: (a) 0.2 L/min, (b) 0.35 L/min, (c) 0.7 L/min, (d) 1.4 L/min.

All measured concentrations are quoted after correction for evaporation of the solvent in each case. The error bars represent standard deviation values between three measurements.

RESULTS AND DISCUSSION

NH_3 Production in a System Comprised of N_2 Plasma with H_2O Vapor in Contact with Liquid H_2O . We studied the production of various compounds in liquid by exposing a liquid H_2O sample to the plasma jet effluent for 10 min (Figure 1b), at several feed gas flow rates (Figure 2). The minimal flow rate of 0.2 L/min was chosen to avoid the heat-up of the gas (see SI, Table S1) to temperatures which would lead to thermal evaporation of the plasma-exposed water, and therefore a potential loss of NH_3 due to its decreased solubility at elevated temperatures.³⁷ The maximal flow rate obtainable with the equipment used was 1.4 L/min. In all our experiments, the liquid samples remained at room temperature or slightly above (21 ± 3 °C), due to the relatively low temperature of the plasma effluent at 5 mm from the nozzle and the cooling down of liquid due to evaporation. Using liquid water has several purposes. First, it demonstrates the possibility of using H_2O as a benign solvent for the storage of nitrogen fixation products in our experiments. Second, it enables facile measurements of the generated products by spectrophotometric analysis of the liquid samples. Finally, we studied the role of liquid H_2O in nitrogen fixation (*vide infra*).

NH_3 and $\text{NO}_2^-/\text{NO}_3^-$ are the products of nitrogen fixation with H_2O molecules. H_2O can react with, e.g., N atoms to produce $\cdot\text{NH}$ and $\cdot\text{OH}$ radicals, as proposed by Haruyama et al.²⁸ In addition, H_2O also forms $\cdot\text{OH}$ and H via, e.g., direct electron impact²² or reacting with UV photons of plasma.²⁹ $\cdot\text{OH}$ can further recombine into H_2O_2 .²² H_2O_2 is thus one of

the products in the $\text{N}_2/\text{H}_2\text{O}$ plasma system and must be acknowledged in the overall nitrogen fixation process.

In our experiments, the amounts of formed NO_3^- and H_2O_2 slightly increase up to 20% H_2O saturation but remain the same at ca. 20–100% H_2O saturation, while the concentrations of NH_3 and NO_2^- keep increasing upon higher H_2O saturation. Interestingly, the yields of NH_3 and $\text{NO}_2^-/\text{NO}_3^-$ (i.e., total conversion of N_2) increase with increasing gas flow rate, but not proportionally. For example, at 50% H_2O saturation, the concentration of produced NH_3 increases from ca. 200 μM to 400 μM for gas flow rates rising from 0.2 to 1.4 L/min. Similarly, the concentration of NO_2^- is 125 μM and 225 μM for 0.2 and 1.4 L/min. This is attributed to the reduced residence time of the feed gas within the plasma ignition region, while the plasma frequency remains the same (Figure S1). Therefore, a lower feed gas flow rate is preferable for a higher conversion.

In spite of the higher production at higher H_2O vapor content (50–100%), the selectivity toward NH_3 decreases at high contents of H_2O vapor at all flow rates, down to 60–70%, compared to 70–80% with dry N_2 (Figure 2; see also Table S2). However, at low H_2O vapor content (approximately 2–10% saturation), it increases compared to the dry N_2 feed gas, and it is around 90% with any of the N_2 flow rates. Remarkably, with 0.2 L/min of N_2 gas and 5% H_2O vapor saturation, the selectivity toward NH_3 is ca. 96% (Figure 2a, Table S2). In other words, the introduction of small amounts of H_2O vapor yield both higher NH_3 production rate and higher selectivity. Larger amounts of H_2O vapor further increase the production rate, albeit with lower selectivity.

Nonetheless, the introduction of H_2O vapor into the plasma feed gas clearly had two main effects: (i) increased total N_2

Table 1. Comparative Summary of Our Work with Other Studies on NH₃ Production by N₂ Plasmas in Contact with H₂O

NH ₃ production			N ₂ conversion (%)	additional experimental features	ref ^a
rate (mg/h)	selectivity (%)	energy consumption (MJ/mol)			
0.440	>99	139	0.0059	electrolytic system (ground electrode in H ₂ O), closed reactor, low pH	27
2.295	<1	n/a ^b	0.042	separate UV source, open reactor	31
n/a	69	962	n/a	separate UV source, closed reactor	28
0.033	n/a	n/a	n/a	separate UV source, closed reactor	29
0.143	45	n/a	0.0003	separate UV source, air-free atmosphere	30
0.064	95	95	0.0008	open reactor, no additional electrolytic or UV components	this work

^aThe values calculated here correspond to the reported conditions with the highest selectivity of NH₃ production. ^bThe absence of necessary experimental details did not allow calculation of the numerical values.

conversion (with all H₂O vapor contents) compared to dry N₂ interacting with liquid H₂O and (ii) increased selectivity toward NH₃ (at low H₂O vapor content).

We also calculated the energy consumption (as explained in the SI, T5 Energy Consumption Calculation), yielding values in our noncatalytic, H₂-free plasma system of 95–118 MJ/mol NH₃ at 0.2 L/min N₂ and 5–10% H₂O vapor saturation (i.e., the conditions giving the highest NH₃ selectivity). This is in the range of plasma-catalytic processes using N₂ and pure H₂, reporting values from ca. 2 to 600 MJ/mol NH₃.^{23,44} It is worth noting that despite the low energy cost of H₂ production, e.g., from H₂O via electrolysis (<1 MJ/mol⁴⁵), the produced H₂ must be stored and delivered into a reactive system, and H₂ storage is a bottleneck and potentially a “showstopper” for an H₂ economy.⁴⁶ In contrast, we demonstrate the possibility of the direct, “one-pot” synthesis of NH₃ from the gases N₂ and H₂O.

Furthermore, the calculated energy consumption of total N₂ fixation was 92–105 MJ per mole of converted N₂ for the conditions specified above, and only 15 MJ/mol for the conditions which afforded the highest total concentration of NH₃ and NO₂⁻/NO₃⁻ (1.4 L/min N₂, 100% H₂O saturation), albeit with somewhat lower selectivity.

We also assessed the energy efficiency of the process. For this, we calculated the ΔG values for a hypothetical reaction of N₂ with H₂O leading to NH₃ under the conditions which afford the highest NH₃ selectivity (i.e., 2N₂ + 6H₂O → 3O₂ + 4NH₃, see Mechanistic Considerations below). ΔG was calculated for two “envelope” temperature values (298 and 1623 K/1350 °C as the lowest and highest possible temperatures in our system, see Table S1) and the partial pressures of the products and reactants calculated from the conversion and yield values (see Table S2). The detailed description of the ΔG calculation is found in the SI, T6 Calculation of ΔG Values. In short, based on the energy consumption obtained in our work (around 100 MJ/mol) and the ΔG of ca. 1 MJ/mol (see T6 Calculation of ΔG Values in the SI), we achieve an energy efficiency of ca. 1% for NH₃ production. Thus, it is clear that there is still room for improvement via, e.g., optimization of the reaction parameters or the plasma setup. However, as stated by Chen et al., although using H₂O as a feedstock is slightly more energy demanding than H₂, avoiding the HB and using milder conditions for NH₃ production can become overall energetically favorable.⁴⁷

Besides NH₃, NO₃⁻/NO₂⁻, and H₂O₂, we also analyzed the solutions for NH₂OH and NH₂NH₂, potential products of the complex chemistry in N₂/H₂O plasmas⁴⁸ (see Figure S8 and

details on the analysis selectivity in the SI). We detected no NH₂OH or NH₂NH₂ under all conditions investigated, but we stress that only assessing the full range of the possible N₂ fixation products allows evaluating the production selectivity. We acknowledge that a separation of NH₃, NO₂⁻, and NO₃⁻ may result in an extra energy cost. However, (i) under optimized conditions, the selectivity in our case was over 95%, and (ii) the separation is possible via, e.g., electrophoresis.⁴⁹ Therefore, both the N₂ fixation and the product separation comply with the concept of electrification of the chemical industry.^{4,50,51}

We also studied the production of the chemical compounds over time under representative conditions: minimal and maximal gas flow rate and low and high vapor saturation. Within the experimental time frame (10 min), the accumulation of all compounds was practically linear (Figure S9), indeed allowing comparison of production rates. This suggests that despite the pH increase (max. up to 8–8.5 under all conditions), NH₃ was continuously induced in the plasma-exposed water and remained dissolved in it. This was also confirmed by an experiment in which the jet and the reaction vessel with H₂O were contained inside a gastight reactor,^{33,39} with the reactor exhaust passing through a second H₂O sample (Figure S5). We did not observe any detectable amounts of NH₃, NO₃⁻/NO₂⁻, or H₂O₂ in the second sample, confirming that all (or most) products of N₂ fixation remained in the plasma-exposed solution.

It must be acknowledged that using a reactor with static (i.e., nonmoving) liquid can have diffusion-related limitations,⁵² such as accumulation of the products in the upper layers of the liquid, and associated dominance of secondary reactions in the liquid phase. While we did not observe a decrease of the rate of absorption of the N₂ fixation products in our experiments, a potential alternative in future investigations would be a reactor where the gaseous plasma would be in contact with a flowing liquid.¹⁴

The conversion of N₂ under all conditions remained rather low, as is common for N₂/H₂O plasma systems (Table 1). The highest conversion observed corresponds to the lowest flow rate of N₂ (0.2 L/min), as discussed above, reaching a maximum of 0.0023% (see Table S2 for the full list of calculated conversion values). While the N₂ conversion/NH₃ production rate in our work is somewhat lower than in some of the other studies reported in the literature for N₂ plasma in contact with H₂O, the advantage of our setup is the simple design, i.e., open reactor with no additional electrolytic or UV components, which of course add in the NH₃ production. In addition, the NH₃ selectivity and energy consumption in our

work is generally better than the values reported in the literature (see Table 1).

Mechanistic Considerations. To understand the pathways leading to NH_3 , we can consider several possibilities. N_2 molecules can be converted in the plasma into electronically or vibrationally excited states (e.g., N_2^* , $\text{N}_2(\nu)$), N_2^+ ions, and N atoms, as shown by Sakakura et al.³⁰ These species further interact with H_2O (or H and $\cdot\text{OH}$ generated from H_2O by plasma), forming first $\cdot\text{NH}$ and ultimately NH_3 .^{28–30} On the other hand, H atoms (again generated from H_2O via interaction with plasma) can also directly interact with N_2 molecules, also yielding NH_3 .²⁷ As for the plasma action, the key reactions are direct electron impact excitation and dissociation of N_2 and H_2O .^{22,48} Additionally, UV irradiation from plasma may assist in dissociation of H_2O into H and $\cdot\text{OH}$.^{28,29}

Our experiments suggest that the reaction regimes can be divided into three main groups, depending on the H_2O saturation of the N_2 gas. In the first regime, dry N_2 reacts with the plasma-exposed H_2O . At higher flow rates of N_2 , nearly equal amounts of NH_3 and H_2O_2 are formed (Figure 2c,d), suggesting interaction of, e.g., N atoms with H_2O to produce $\cdot\text{NH}$ and $\cdot\text{OH}$ and further recombination of $\cdot\text{OH}$ into H_2O_2 . Here, the plasma can interact with the liquid phase H_2O molecules as suggested in the literature.^{28–30} However, it has also been suggested that plasma interacts first with a vapor layer immediately above the liquid surface.^{31,52,53} This agrees with our previous results, where we experimentally demonstrated that the plasma effluent does not interact directly with the liquid but instead reacts with the vapor above the solvent.³⁴ More precise evaluations require physicochemical modeling.

The second regime (2–10% H_2O saturation) yields NH_3 with high selectivity. The absence of extra amounts of H_2O_2 suggests that another species potentially formed from O in H_2O in this regime is O_2 , or possibly N_2O , which were not analyzed in this study. N_2O , however, could react with $\cdot\text{OH}$ to be transformed back into N_2 .⁵⁴

The third regime (N_2 saturation with H_2O vapor of 20% and above) exhibits the formation of NH_3 and $\text{NO}_2^- + \text{NO}_3^-$ in a ratio close to 2:1. This regime is possibly controlled by the initial formation of NH_3 (similarly to the second regime) and its further oxidation. However, Sakakura et al. proposed that this could be due to the reactions of N with H_2O and/or H (from H_2O) leading to NH_3 , and N with $\cdot\text{OH}$ (from H_2O) leading to $\text{NO}_2^-/\text{NO}_3^-$.³⁰

Thus, in all regimes, the formation of the reduced product NH_3 is accompanied by the formation of an oxidized one, the nature of which likely depends on the regime (i.e., $\text{NO}_2^-/\text{NO}_3^-$ (from N_2); H_2O_2 or O_2 (from H_2O)). In any regime, H_2O is a key component since it is the only source of H for NH_3 . The interaction of plasma with H_2O in the feed gas and H_2O exposed to the effluent is an important parameter of the described reactive system.

Influence of Ambient Air on NH_3 Production. The use of an air-free gastight reactor in which the gaseous atmosphere consisted only of the feed gas ($\text{N}_2 + \text{H}_2\text{O}$) and the solvent vapor (H_2O) allowed us to evaluate the influence of the ambient atmosphere on NH_3 synthesis. Generally, in plasmas with an active effluent (i.e., containing high energy species, such as electrons), the chemistry is strongly affected by the composition of gas in contact with the effluent.^{34,52} Ambient air can diffuse into the effluent, altering the production of chemical species.^{22,43} However, comparing the experiments in

the reactor and the open reaction vessel revealed no significant differences in product concentrations (Figure 3), probably due

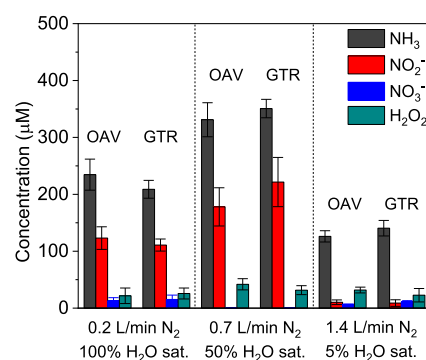


Figure 3. Concentration of produced NH_3 , NO_3^- , NO_2^- , and H_2O_2 in liquid H_2O in an open atmosphere in a reaction vessel (OAV) and in an air-free, gastight reactor (GTR), under three representative plasma conditions.

to the high gas velocity, reasonably short distance between jet and liquid, and the walls of the reaction vessel reducing the air diffusion. This emphasizes the facile use of our experimental setup for NH_3 production, and its independence from the surrounding air eliminates the need for an air-free reactor.^{27,29}

NH_3 Production When Using Air As the Feed Gas. Using air instead of N_2 as the feed gas expectedly provided very different results. With dry air, detectable amounts of NH_3 were produced only with a 0.7–1.4 L/min flow rate (Figure 4).

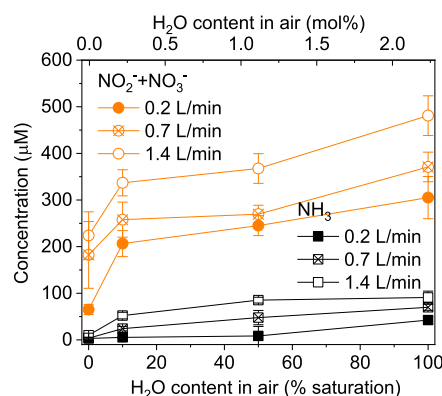


Figure 4. Concentration of produced NH_3 and $\text{NO}_2^- + \text{NO}_3^-$ in liquid H_2O from air plasma, as a function of H_2O vapor saturation.

Introducing H_2O vapor into the plasma feed gas, we observed higher NH_3 formation under all conditions. It was higher at higher flow rates, like in the N_2 plasma (Figure 2). However, the amount of produced NH_3 was ca. 6 times lower than in the N_2 plasma with the same flow rates. For instance, the concentration of produced NH_3 in H_2O with a gas flow rate of 0.2 L/min was ca. 40 and 240 μM with the air and N_2 plasma, respectively (see Figure 2a). Moreover, the NH_3 selectivity dropped drastically when using air plasma. In all cases, the total concentration of NO_3^- and NO_2^- produced by air plasma was 5–6 times higher than the concentration of NH_3 (see Figure 4), reducing the NH_3 selectivity to values below 15–20%. Nonetheless, the total yield of all products of nitrogen fixation evidently increased upon the addition of H_2O vapor with air as a feed gas, as well as with N_2 , making the process more efficient. However, the results strongly indicate

that N_2 as the plasma feed gas is required to achieve high NH_3 selectivity.

Contribution of H_2O Vapor and Plasma-Exposed H_2O to NH_3 Formation. Because this is the first work describing the use of H_2O vapor in the plasma feed gas, we needed to elucidate whether the gaseous plasma effluent interacted with the plasma-exposed H_2O or the NH_3 was produced from H_2O vapor. To evaluate the first option, the distance between the plasma jet and the liquid has to be increased to exclude interaction with the liquid. This could result in a potential loss of NH_3 due to the effluent dissipation into the gas phase instead of delivering NH_3 into the liquid (the increase of the effluent width, and hence the decrease of the gas velocity, within the 5 mm distance from the jet is shown in Table S1). To avoid a drastic drop in the gas velocity, we performed experiments in which the tip of the plasma jet was inserted into a glass tube (see the Experimental Section). The opposite end of the glass tube (ID 1 mm) was positioned 2 mm above the liquid (Figure S6). Plasma was ignited with N_2 and H_2O vapor as the feed gas. The total distance from the plasma jet was ca. 300 mm.

Comparing Figure 5 and Figure 2a, it is seen that the concentrations of NH_3 and NO_3^-/NO_2^- are slightly lower

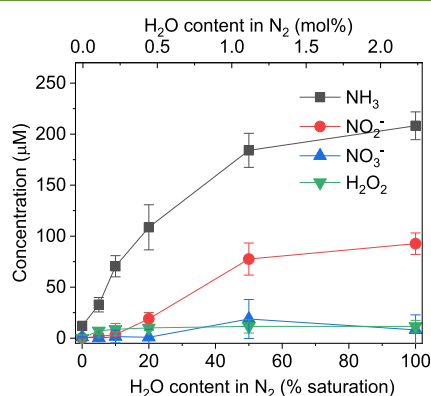


Figure 5. Concentration of produced NH_3 , NO_3^- , NO_2^- , and H_2O_2 in liquid H_2O , with 0.2 L/min N_2 , as a function of H_2O vapor saturation, when using a glass tube to increase the distance between the plasma jet and liquid without a drop in gas velocity.

than the values in H_2O exposed to plasma at a 5 mm distance, at all H_2O saturation values (5–100%). For example, at 50% H_2O saturation, the NH_3 concentrations are ca. 190 μM at a 300 mm distance, compared to 210 μM at a 5 mm distance. At the same time, the NH_3 selectivity remains practically the same, suggesting similar reaction pathways. The H_2O_2 concentrations were substantially lower here, suggesting that most H_2O_2 was formed via interaction of the effluent with the plasma-exposed H_2O . In other words, H_2O_2 is largely formed via recombination of $\bullet OH$ formed from plasma-exposed H_2O upon interaction with the plasma effluent, while NH_3 , NO_3^- , and NO_2^- are mainly formed upon reaction of N_2 molecules (or excited species) with H and $\bullet OH$ originating from H_2O vapor in the feed gas, rather than from the plasma-exposed liquid H_2O .

A notable difference, however, was observed for dry N_2 . Here, virtually no NO_3^-/NO_2^- or NH_3 was detected. This is expected, because no H source was present in the system. The considerable production of NH_3 with dry N_2 at 5 mm (Figure 2) suggests that the plasma effluent does interact with H_2O of

the solvent under those conditions. With increasing H_2O content in the plasma feed gas, this interaction becomes less pronounced. We hypothesize that this is due to the lower density of electrons and excited N_2 molecules and atoms in the effluent with high H_2O vapor admixtures in the feed gas.^{22,34} Still, even at 100% saturation of the feed gas, the NH_3 , NO_3^- , and NO_2^- concentrations were slightly lower with no effluent-solvent interaction (i.e., lower at 300 mm than at 5 mm), indicating that these products are also formed to a minor extent from the plasma-exposed liquid H_2O .

At a high flow rate, the interaction of the plasma effluent with the liquid H_2O is more probable. However, we observed similar effects with 1.4 L/min (see Figure S10 and Figure 2d). The addition of H_2O vapor to the feed gas reduces the effect of the effluent interaction with the molecules of the plasma-exposed H_2O but does not eliminate it completely. This suggests that in our plasma jet, most of the chemistry leading to NH_3 (and NO_2^-/NO_3^-) formation occurs in the gas phase plasma, via reactions of the feed gas components, with only a minor contribution from the H_2O molecules of the solvent, either liquid or evaporated.

This hypothesis was further confirmed by experiments with isotopically labeled water. We used (1) a D_2O liquid sample exposed to H_2O vapor plasma, (2) H_2O liquid exposed to D_2O vapor plasma, and (3) D_2O liquid exposed to D_2O vapor plasma (Figure 6). This was done to distinguish between the

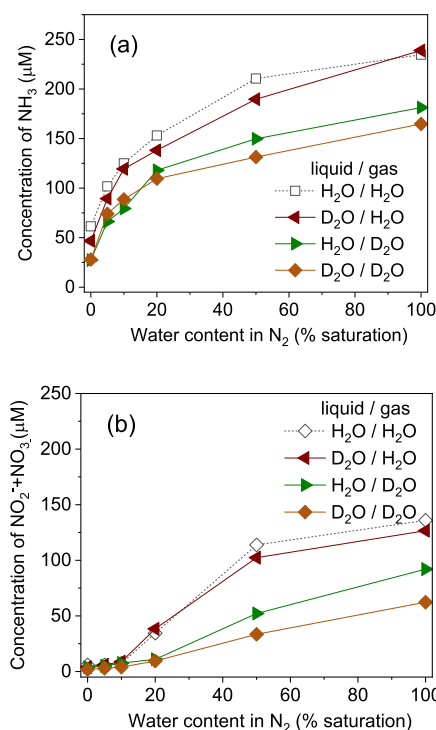


Figure 6. Concentration of produced (a) NH_3 and (b) $NO_2^- + NO_3^-$ in liquid water, as a function of water vapor saturation, with 0.2 L/min N_2 flow rate, for different combinations of liquid/gas H_2O/D_2O .

water vapor in the feed gas and water of the exposed sample. The results were compared with the data with H_2O liquid and H_2O vapor (added as dashed lines in Figure 6).

When the liquid was changed to D_2O but the plasma feed gas contained H_2O vapor, the NH_3 and $NO_3^- + NO_2^-$ concentrations remain virtually the same as with liquid H_2O . This means that both the NH_3 production rate and selectivity

were the same. Switching from H₂O to D₂O introduces the primary kinetic isotope effect (KIE),⁵⁵ which could lead to potentially different concentrations of the N₂ fixation products. Indeed, a reactive system comprised of D₂O vapor and exposed D₂O liquid yielded lower NH₃ and NO₃⁻ + NO₂⁻ concentrations, although the selectivity remained the same. This was in agreement with our previous studies on plasmas with isotopically labeled water^{33,34} and the work of Haruyama et al.²⁸ When the liquid H₂O sample was exposed to D₂O vapor-containing N₂ plasma, the concentrations of both NH₃ and NO₂⁻/NO₃⁻ decreased compared to the H₂O liquid/H₂O vapor conditions (again, with the same selectivity), but they were slightly higher than those in the case of D₂O liquid/D₂O vapor. With D₂O liquid/H₂O vapor, the difference was probably too small to be observed. Nonetheless, these data confirm that liquid H₂O participates in the NH₃ and NO₃⁻ + NO₂⁻ production to some (minor) extent, as we hypothesized above (*vide infra*), but that water (H₂O or D₂O) introduced as a vapor component plays a much larger role than the plasma-exposed liquid.

CONCLUSIONS

We present here for the first time a green NH₃ synthesis process, based on noncatalytic nitrogen fixation by non-equilibrium plasma using H₂O vapor instead of H₂. We used a very simple plasma setup for a straightforward on-spot generation of NH₃ in a benign solvent (H₂O), avoiding more complex air-free plasma chambers. We assess the formation of the full range of possible N₂ fixation products, which is required to evaluate the selectivity of NH₃ formation. We characterized the plasma jet using optical emission and Rayleigh scattering spectroscopy, time-resolved ICCD imaging, and current–voltage analysis. We also evaluated the selectivity and applicability of the colorimetric analytical techniques used to measure the concentrations of the N₂ fixation products in H₂O.

We studied the selectivity and rate of NH₃ production as a function of the added H₂O vapor content in the plasma feed gas operated at different flow rates. Excellent selectivity of NH₃ formation (up to 96%) and increased production rate compared to dry N₂ in contact with liquid H₂O (up to 0.064 mg/h) were achieved under conditions with low amounts of H₂O vapor saturation of the N₂ feed gas. With higher H₂O vapor contents, the selectivity was lower (ca. 60–85%), but the combined yield of all N₂ fixation products (i.e., NH₃, NO₃⁻, NO₂⁻) increased. Similarly, the total N₂ fixation product yield increased when air was used instead of N₂, but the selectivity toward NH₃ was drastically lower when compared to the N₂ feed gas. Thus, in terms of the total N₂ fixation efficiency, higher levels of H₂O vapor saturation of the plasma feed gas were beneficial as they increased the overall N₂ conversion. Notably, the energy consumption of the presented catalyst-free and H₂-free plasma system (around 100 MJ/mol for NH₃, or 15 MJ/mol for total N₂ fixation) are in the range of reported values of plasma-assisted catalytic NH₃ production, but with the additional advantage of using H₂O vapor and the absence of a catalyst.

Experiments without direct plasma–liquid interaction and with isotopically labeled water were performed to study the contribution of H₂O vapor in the feed gas and liquid H₂O. The results show some interaction of plasma effluent with the plasma-exposed H₂O, but the role of this interaction decreases

dramatically when H₂O vapor is introduced into the N₂ feed gas.

Therefore, using H₂O vapor admixtures in N₂ can result in both a higher NH₃ selectivity and production rate. At the same time, it reduces the need to use liquid water as a reagent, enabling the use of plasma setups without a direct plasma–liquid interaction. Future studies in this field, including optimization of the plasma setup and development of computational models, can shed more light on the mechanisms leading to NH₃ and other N₂ fixation products. This can further enhance the energy efficiency, selectivity, and yield outcomes.

ASSOCIATED CONTENT

Supporting Information

The Supporting Information is available free of charge at <https://pubs.acs.org/doi/10.1021/acssuschemeng.9b07849>.

Additional details on plasma setup characterization, analytical techniques used, and further experimental data (PDF)

AUTHOR INFORMATION

Corresponding Author

Yury Gorbanev – Research Group PLASMANT, Department of Chemistry, University of Antwerp, 2610 Wilrijk, Belgium; orcid.org/0000-0002-8059-4464; Phone: +32(0) 32652343; Email: yury.gorbanev@uantwerpen.be

Authors

Elise Vervloessem – Research Group PLASMANT, Department of Chemistry, University of Antwerp, 2610 Wilrijk, Belgium; Research Unit Plasma Technology (RUPT), Department of Physics, Ghent University, 9000 Ghent, Belgium
Anton Nikiforov – Research Unit Plasma Technology (RUPT), Department of Physics, Ghent University, 9000 Ghent, Belgium
Annemie Bogaerts – Research Group PLASMANT, Department of Chemistry, University of Antwerp, 2610 Wilrijk, Belgium; orcid.org/0000-0001-9875-6460

Complete contact information is available at: <https://pubs.acs.org/doi/10.1021/acssuschemeng.9b07849>

Author Contributions

The manuscript was written through contributions of all authors. All authors have given approval to the final version of the manuscript.

Funding

This research was supported by the Excellence of Science FWO-FNRS project (FWO grant ID GoF9618n, EOS ID 30505023), the Catalisti Moonshot project P2C, and the Methusalem project of the University of Antwerp.

Notes

The authors declare no competing financial interest.

ACKNOWLEDGMENTS

We would like to thank Sylvia Dewilde (Department of Biomedical Sciences) for providing analytical equipment.

ABBREVIATIONS

HB, Haber-Bosch process; ID, internal diameter; OD, outer diameter; MFC, mass flow controller; OAV, open atmosphere reaction vessel; GTR, air-free gastight reactor

REFERENCES

- (1) Hoffman, B. M.; Lukoyanov, D.; Yang, Z.-Y.; Dean, D. R.; Seefeldt, L. C. Mechanism of Nitrogen Fixation by Nitrogenase: The Next Stage. *Chem. Rev.* **2014**, *114* (8), 4041–4062.
- (2) Pfromm, P. H. Towards sustainable agriculture: Fossil-free ammonia. *J. Renewable Sustainable Energy* **2017**, *9* (3), 034702–034712.
- (3) Erisman, J. W.; Sutton, M. A.; Galloway, J.; Klimont, Z.; Winiwarter, W. How a century of ammonia synthesis changed the world. *Nat. Geosci.* **2008**, *1* (10), 636–639.
- (4) Li, S.; Medrano Jimenez, J.; Hessel, V.; Gallucci, F. Recent Progress of Plasma-Assisted Nitrogen Fixation Research: A Review. *Processes* **2018**, *6* (12), 248–272.
- (5) Oldroyd, G. E. D.; Dixon, R. Biotechnological solutions to the nitrogen problem. *Curr. Opin. Biotechnol.* **2014**, *26*, 19–24.
- (6) U.S. Geological Survey. *Mineral Commodity Summaries 2019*; U.S. Department of the Interior, 2019; pp 116–117. Available online at <https://www.usgs.gov/centers/nmic/mineral-commodity-summaries> (accessed 2019.11.20).
- (7) Kandemir, T.; Schuster, M. E.; Senyshyn, A.; Behrens, M.; Schlögl, R. The Haber–Bosch Process Revisited: On the Real Structure and Stability of “Ammonia Iron” under Working Conditions. *Angew. Chem., Int. Ed.* **2013**, *52* (48), 12723–12726.
- (8) Xie, X.-Y.; Xiao, P.; Fang, W.-H.; Cui, G.; Thiel, W. Probing Photocatalytic Nitrogen Reduction to Ammonia with Water on the Rutile TiO₂ (110) Surface by First-Principles Calculations. *ACS Catal.* **2019**, *9* (10), 9178–9187.
- (9) Cui, X.; Tang, C.; Zhang, Q. A Review of Electrocatalytic Reduction of Dinitrogen to Ammonia under Ambient Conditions. *Adv. Energy Mater.* **2018**, *8* (22), 1800369–1800393.
- (10) Shah, J.; Wang, W.; Bogaerts, A.; Carreon, M. L. Ammonia Synthesis by Radio Frequency Plasma Catalysis: Revealing the Underlying Mechanisms. *ACS Appl. Energy Mater.* **2018**, *1* (9), 4824–4839.
- (11) Bogaerts, A.; Neyts, E.; Gijbels, R.; van der Mullen, J. Gas discharge plasmas and their applications. *Spectrochim. Acta, Part B* **2002**, *57* (4), 609–658.
- (12) Gorbanev, Y.; Privat-Maldonado, A.; Bogaerts, A. Analysis of Short-Lived Reactive Species in Plasma–Air–Water Systems: The Dos and the Do Nots. *Anal. Chem.* **2018**, *90* (22), 13151–13158.
- (13) Adamovich, I.; Baalrud, S D.; Bogaerts, A.; Bruggeman, P J.; Cappelli, M.; Colombo, V.; Czarnetzki, U.; Ebert, U.; Eden, J G; Favia, P.; Graves, D B; Hamaguchi, S; Hieftje, G; Hori, M; Kaganovich, I D; Kortshagen, U; Kushner, M J; Mason, N J; Mazouffre, S; Thagard, S M.; Metelmann, H-R; Mizuno, A; Moreau, E; Murphy, A B; Niemira, B A; Oehrlein, G S; Petrovic, Z L.; Pitchford, L C; Pu, Y-K; Rauf, S; Sakai, O; Samukawa, S; Starikovskaia, S; Tennyson, J; Terashima, K; Turner, M M; van de Sanden, M C M; Vardelle, A The 2017 Plasma Roadmap: Low temperature plasma science and technology. *J. Phys. D: Appl. Phys.* **2017**, *50* (32), 323001–323046.
- (14) Gorbanev, Y.; Leifert, D.; Studer, A.; O’Connell, D.; Chechik, V. Initiating radical reactions with non-thermal plasmas. *Chem. Commun.* **2017**, *53* (26), 3685–3688.
- (15) Zhou, R.; Zhou, R.; Prasad, K.; Fang, Z.; Speight, R.; Bazaka, K.; Ostrikov, K. Cold atmospheric plasma activated water as a prospective disinfectant: the crucial role of peroxydinitrite. *Green Chem.* **2018**, *20* (23), 5276–5284.
- (16) Puač, N.; Gherardi, M.; Shiratani, M. Plasma agriculture: A rapidly emerging field. *Plasma Processes Polym.* **2018**, *15* (2), 1700174–1700178.
- (17) Privat-Maldonado, A.; Gorbanev, Y.; Dewilde, S.; Smits, E.; Bogaerts, A. Reduction of Human Glioblastoma Spheroids Using Cold Atmospheric Plasma: The Combined Effect of Short- and Long-Lived Reactive Species. *Cancers* **2018**, *10* (11), 394–410.
- (18) Mehta, P.; Barboun, P.; Herrera, F. A.; Kim, J.; Rumbach, P.; Go, D. B.; Hicks, J. C.; Schneider, W. F. Overcoming ammonia synthesis scaling relations with plasma-enabled catalysis. *Nat. Catal.* **2018**, *1* (4), 269–275.
- (19) Barboun, P.; Mehta, P.; Herrera, F. A.; Go, D. B.; Schneider, W. F.; Hicks, J. C. Distinguishing Plasma Contributions to Catalyst Performance in Plasma-Assisted Ammonia Synthesis. *ACS Sustainable Chem. Eng.* **2019**, *7* (9), 8621–8630.
- (20) Mehta, P.; Barboun, P.; Go, D. B.; Hicks, J. C.; Schneider, W. F. Catalysis Enabled by Plasma Activation of Strong Chemical Bonds: A Review. *ACS Energy Lett.* **2019**, *4* (5), 1115–1133.
- (21) Rouwenhorst, K. H. R.; Kim, H.-H.; Lefferts, L. Vibrationally Excited Activation of N₂ in Plasma-Enhanced Catalytic Ammonia Synthesis: A Kinetic Analysis. *ACS Sustainable Chem. Eng.* **2019**, *7* (20), 17515–17522.
- (22) Fridman, A. *Plasma Chemistry*; Cambridge University Press: Cambridge, UK, 2008.
- (23) Bogaerts, A.; Neyts, E. C. Plasma Technology: An Emerging Technology for Energy Storage. *ACS Energy Lett.* **2018**, *3* (4), 1013–1027.
- (24) Peng, P.; Chen, P.; Schiappacasse, C.; Zhou, N.; Anderson, E.; Chen, D.; Liu, J.; Cheng, Y.; Hatzenbeller, R.; Addy, M.; Zhang, Y.; Liu, Y.; Ruan, R. A review on the non-thermal plasma-assisted ammonia synthesis technologies. *J. Cleaner Prod.* **2018**, *177*, 597–609.
- (25) Hong, J.; Prawer, S.; Murphy, A. B. Plasma Catalysis as an Alternative Route for Ammonia Production: Status, Mechanisms, and Prospects for Progress. *ACS Sustainable Chem. Eng.* **2018**, *6* (1), 15–31.
- (26) Kumari, S.; Pishgar, S.; Schwarting, M. E.; Paxton, W. F.; Spurgeon, J. M. Synergistic plasma-assisted electrochemical reduction of nitrogen to ammonia. *Chem. Commun.* **2018**, *54* (95), 13347–13350.
- (27) Hawtof, R.; Ghosh, S.; Guarr, E.; Xu, C.; Mohan Sankaran, R.; Renner, J. N. Catalyst-free, highly selective synthesis of ammonia from nitrogen and water by a plasma electrolytic system. *Sci. Adv.* **2019**, *5* (1), No. eaat5778.
- (28) Haruyama, T.; Namise, T.; Shimoshimizu, N.; Uemura, S.; Takatsuji, Y.; Hino, M.; Yamasaki, R.; Kamachi, T.; Kohno, M. Non-catalyzed one-step synthesis of ammonia from atmospheric air and water. *Green Chem.* **2016**, *18* (16), 4536–4541.
- (29) Sakakura, T.; Uemura, S.; Hino, M.; Kiyomatsu, S.; Takatsuji, Y.; Yamasaki, R.; Morimoto, M.; Haruyama, T. Excitation of H₂O at the plasma/water interface by UV irradiation for the elevation of ammonia production. *Green Chem.* **2018**, *20* (3), 627–633.
- (30) Sakakura, T.; Murakami, N.; Takatsuji, Y.; Morimoto, M.; Haruyama, T. Contribution of Discharge Excited Atomic N, N₂^{*}, and N₂⁺ to a Plasma/Liquid Interfacial Reaction as Suggested by Quantitative Analysis. *ChemPhysChem* **2019**, *20* (11), 1467–1474.
- (31) Peng, P.; Chen, P.; Addy, M.; Cheng, Y.; Zhang, Y.; Anderson, E.; Zhou, N.; Schiappacasse, C.; Hatzenbeller, R.; Fan, L.; Liu, S.; Chen, D.; Liu, J.; Liu, Y.; Ruan, R. In situ plasma-assisted atmospheric nitrogen fixation using water and spray-type jet plasma. *Chem. Commun.* **2018**, *54* (23), 2886–2889.
- (32) Clarke, C. J.; Tu, W.-C.; Levers, O.; Bröhl, A.; Hallett, J. P. Green and Sustainable Solvents in Chemical Processes. *Chem. Rev.* **2018**, *118* (2), 747–800.
- (33) Gorbanev, Y.; Verlact, C. C. W.; Tinck, S.; Tuenter, E.; Foubert, K.; Cos, P.; Bogaerts, A. Combining experimental and modelling approaches to study the sources of reactive species induced in water by the COST RF plasma jet. *Phys. Chem. Chem. Phys.* **2018**, *20* (4), 2797–2808.
- (34) Gorbanev, Y.; O’Connell, D.; Chechik, V. Non-Thermal Plasma in Contact with Water: The Origin of Species. *Chem. - Eur. J.* **2016**, *22*, 3496–3505.
- (35) Kaushik, N.; Uddin, N.; Sim, G. B.; Hong, Y. J.; Baik, K. Y.; Kim, C. H.; Lee, S. J.; Kaushik, N. K.; Choi, E. H. Responses of Solid Tumor Cells in DMEM to Reactive Oxygen Species Generated by Non-Thermal Plasma and Chemically Induced ROS Systems. *Sci. Rep.* **2015**, *5*, 8587–8597.
- (36) Ananth, A.; Dharaneedharan, S.; Seo, H.-J.; Heo, M.-S.; Boo, J.-H. Soft jet plasma-assisted synthesis of Zinc oxide nanomaterials: Morphology controls and antibacterial activity of ZnO. *Chem. Eng. J.* **2017**, *322*, 742–751.

- (37) Lide, D. R. *CRC Handbook of Chemistry and Physics*; CRC Press: Boca Raton, FL, 1992.
- (38) Akishev, Y. S.; Aponin, G. I.; Grushin, M. E.; Karal'nik, V. B.; Monich, A. E.; Pan'kin, M. V.; Trushkin, N. I. Development of a spark sustained by charging the stray capacitance of the external circuit in atmospheric-pressure nitrogen. *Plasma Phys. Rep.* **2007**, *33* (7), 584–601.
- (39) Gorbanev, Y.; Soriano, R.; O'Connell, D.; Chechik, V. An Atmospheric Pressure Plasma Setup to Investigate the Reactive Species Formation. *J. Visualized Exp.* **2016**, *117* (117), No. e54765.
- (40) Bolleter, W. T.; Bushman, C. J.; Tidwell, P. W. Spectrophotometric Determination of Ammonia as Indophenol. *Anal. Chem.* **1961**, *33* (4), 592–594.
- (41) Hu, B.; Tian, X. L.; Shi, W. N.; Zhao, J. Q.; Wu, P.; Mei, S. T. Spectrophotometric determination of hydroxylamine in biological wastewater treatment processes. *Int. J. Environ. Sci. Technol.* **2018**, *15* (2), 323–332.
- (42) Watt, G. W.; Chrisp, J. D. Spectrophotometric Method for Determination of Hydrazine. *Anal. Chem.* **1952**, *24* (12), 2006–2008.
- (43) Van Boxem, W.; Van der Paal, J.; Gorbanev, Y.; Vanuytsel, S.; Smits, E.; Dewilde, S.; Bogaerts, A. Anti-cancer capacity of plasma-treated PBS: effect of chemical composition on cancer cell cytotoxicity. *Sci. Rep.* **2017**, *7* (1), 16478–16492.
- (44) Kim, H.-H.; Teramoto, Y.; Ogata, A.; Takagi, H.; Nanba, T. Atmospheric-pressure nonthermal plasma synthesis of ammonia over ruthenium catalysts. *Plasma Processes Polym.* **2017**, *14* (6), 1600157–1600165.
- (45) *Fuel Cell Technologies Office Multi-Year Research, Development, and Demonstration Plan, Section 3.1: Hydrogen Production*; U.S. Department of Energy, 2015; p 11. Available online at https://www.energy.gov/sites/prod/files/2015/06/f23/fcto_myrrdd_production.pdf (accessed 2019.12.22).
- (46) Service, R. F. The Hydrogen Backlash. *Science* **2004**, *305* (5686), 958–961.
- (47) Chen, J. G.; Crooks, R. M.; Seefeldt, L. C.; Bren, K. L.; Bullock, R. M.; Darensbourg, M. Y.; Holland, P. L.; Hoffman, B.; Janik, M. J.; Jones, A. K.; Kanatzidis, M. G.; King, P.; Lancaster, K. M.; Lymar, S. V.; Pfomm, P.; Schneider, W. F.; Schrock, R. R. Beyond fossil fuel-driven nitrogen transformations. *Science* **2018**, *360* (6391), No. eaar6611.
- (48) Uhm, H. S. Generation of various radicals in nitrogen plasma and their behavior in media. *Phys. Plasmas* **2015**, *22* (12), 123506–123512.
- (49) Padaraukas, A.; Olšauskaite, V.; Paliulionyte, V.; Pranaityte, B. Simultaneous separation of nitrate, nitrite and ammonium by capillary electrophoresis. *Chromatographia* **2000**, *52* (3), 133–136.
- (50) Chen, C.; Lu, Y.; Banares-Alcantara, R. Direct and indirect electrification of chemical industry using methanol production as a case study. *Appl. Energy* **2019**, *243*, 71–90.
- (51) Wang, W.; Patil, B.; Heijkers, S.; Hessel, V.; Bogaerts, A. Nitrogen Fixation by Gliding Arc Plasma: Better Insight by Chemical Kinetics Modelling. *ChemSusChem* **2017**, *10* (10), 2145–2157.
- (52) Bruggeman, P J; Kushner, M J; Locke, B R; Gardeniers, J G E; Graham, W G; Graves, D B; Hofman-Caris, R C H M; Maric, D; Reid, J P; Ceriani, E; Fernandez Rivas, D; Foster, J E; Garrick, S C; Gorbanev, Y; Hamaguchi, S; Iza, F; Jablonowski, H; Klimova, E; Kolb, J; Krcma, F; Lukes, P; Machala, Z; Marinov, I; Mariotti, D; Mededovic Thagard, S; Minakata, D; Neyts, E C; Pawlat, J; Petrovic, Z L; Pflieger, R; Reuter, S; Schram, D C; Schroter, S; Shiraiwa, M; Tarabova, B; Tsai, P A; Verlet, J R R; von Woedtke, T; Wilson, K R; Yasui, K; Zvereva, G Plasma-liquid interactions: a review and roadmap. *Plasma Sources Sci. Technol.* **2016**, *25* (5), 053002–053060.
- (53) Kelly, S.; Turner, M. M. Atomic oxygen patterning from a biomedical needle-plasma source. *J. Appl. Phys.* **2013**, *114* (12), 123301–123308.
- (54) Tsang, W.; Herron, J. T. Chemical Kinetic Data Base for Propellant Combustion I. Reactions Involving NO, NO₂, HNO, HNO₂, HCN and N₂O. *J. Phys. Chem. Ref. Data* **1991**, *20* (4), 609–663.
- (55) Bigeleisen, J.; Mayer, M. G. Calculation of Equilibrium Constants for Isotopic Exchange Reactions. *J. Chem. Phys.* **1947**, *15* (5), 261–267.